


Evidence for Modification of b Quark Hadronization in High-Multiplicity pp Collisions at $\sqrt{s} = 13$ TeV

R. Aaij *et al.**
(LHCb Collaboration)

 (Received 28 April 2022; revised 24 September 2022; accepted 20 January 2023; published 10 August 2023)

The production rate of B_s^0 mesons relative to B^0 mesons is measured by the LHCb experiment in pp collisions at a center-of-mass energy $\sqrt{s} = 13$ TeV over the forward rapidity interval $2 < y < 4.5$ as a function of the charged-particle multiplicity measured in the event. Evidence at the 3.4σ level is found for an increase of the ratio of B_s^0 to B^0 cross sections with multiplicity at transverse momenta below 6 GeV/ c , with no significant multiplicity dependence at higher transverse momentum. Comparison with data from e^+e^- collisions implies that the density of the hadronic medium may affect the production rates of B mesons. This is qualitatively consistent with the emergence of quark coalescence as an additional hadronization mechanism in high-multiplicity collisions.

DOI: [10.1103/PhysRevLett.131.061901](https://doi.org/10.1103/PhysRevLett.131.061901)

Measurements of B mesons at colliders offer unique probes of the hadronization process by which single quarks evolve into color-neutral hadrons. In contrast to light quarks, the large mass of b quarks suppresses their production via nonperturbative processes. In addition, there is no b content in the valence quark distribution of the incoming beam particles [1]. Therefore, production of $b\bar{b}$ pairs at hadron colliders is dominated by hard parton-parton interactions in the initial stages of the collisions and is well described by perturbative QCD calculations [2–4].

The fraction of b quarks that pair with an s quark to form B_s^0 mesons, f_s , and the fraction that pair with a light d quark to form B^0 mesons, f_d , are determined through the hadronization process. One mechanism for hadronization is fragmentation, where showers of partons produced by outgoing quarks form into hadrons [5,6]. Measurements of B hadron production in e^+e^- collisions at the $\Upsilon(5S)$ [7–9] and Z^0 [10–13] resonances give consistent values for the ratio f_s/f_d , which is often interpreted as evidence for the universality of b quark fragmentation assumed by QCD factorization theorems [14]. However, measurements at hadron colliders have shown that the ratio f_s/f_d has a dependence on the collision center-of-mass energy and the B meson transverse momentum p_T [15–19]. The fraction of b quarks which hadronize into baryons also varies with p_T [20,21]. Additionally, recent measurements have shown that charm quark hadronization differs between e^+e^- and

pp collisions [22]. The reason for these variations is not immediately clear and may be explained by hadronization mechanisms other than fragmentation [23].

An alternative hadronization process, quark coalescence, can occur when a quark produced in the collision combines with another quark to form a color singlet hadron. Models incorporating coalescence are successful at reproducing a range of measurements from fixed-target experiments and colliders [24–28]. Coalescence calculations generally require multiple quark wave functions to overlap in position and velocity, so the fraction of hadrons produced by this mechanism is expected to increase with the number of quarks produced in the collision. The effect is expected to be most prominent at relatively low p_T , which is the range where the bulk of the particles created in the collision are found. Coalescence can also lead to enhanced production of baryons at low p_T and is especially important in high-energy heavy ion collisions where a large volume of deconfined quark-gluon plasma (QGP) is formed [29–31]. Data from the CMS Collaboration has shown that B_s^0 production may be enhanced relative to B^+ production in PbPb collisions when compared to pp collisions [32,33]. However, significant uncertainties and the relatively high p_T range covered by that data preclude drawing firm conclusions on the influence of coalescence on B hadronization.

Recent measurements in pp collisions have shown some behaviors similar to those associated with the formation of QGP in collisions of heavy nuclei [34–36]. Among these effects is an enhanced yield of light-quark baryons and mesons with strangeness in collisions where a relatively large number of charged particles are produced [37], which was originally proposed as a QGP signature [38]. If hadronization via coalescence emerges as a mechanism for forming final state B hadrons, then the production rates

*Full author list given at the end of the Letter.

Published by the American Physical Society under the terms of the [Creative Commons Attribution 4.0 International license](https://creativecommons.org/licenses/by/4.0/). Further distribution of this work must maintain attribution to the author(s) and the published article's title, journal citation, and DOI. Funded by SCOAP³.

of B_s^0 hadrons could increase relative to the production of B^0 hadrons as particle multiplicity increases.

This Letter describes LHCb measurements of the ratio of B_s^0 to B^0 cross sections, $\sigma_{B_s^0}/\sigma_{B^0}$, as a function of charged particle multiplicity and p_T . Both the B_s^0 and B^0 candidates are reconstructed through their decays to the $J/\psi\pi^+\pi^-$ final state, where the J/ψ decays into a $\mu^+\mu^-$ pair. This decay mode provides similar yields for both B_s^0 and B^0 mesons. Here, multiplicity is represented by the number of charged tracks reconstructed in a silicon strip detector that surrounds the pp interaction region, the LHCb vertex locator (VELO) detector [39,40]. These measurements use a sample of pp collisions collected at a center-of-mass energy $\sqrt{s} = 13$ TeV, corresponding to an integrated luminosity of 5.4 fb^{-1} .

The LHCb detector is a single-arm forward spectrometer covering the pseudorapidity range $2 < \eta < 5$, described in detail in Refs. [41,42]. Events considered in this analysis are required to satisfy a series of triggers designed to select the decay $J/\psi \rightarrow \mu^+\mu^-$ and have one reconstructed pp interaction point (primary vertex). Each muon candidate is required to penetrate the hadron absorber layers in the LHCb muon system and have $p_T > 500 \text{ MeV}/c$. Candidate J/ψ mesons are formed from pairs of oppositely charged muon candidates that have an invariant mass near the known J/ψ mass and originate from a vertex that is displaced from the primary vertex. Charged pion candidates are identified by the response of the LHCb ring-imaging Cherenkov detectors and are required to have total momentum $p > 3 \text{ GeV}/c$ and transverse momentum $p_T > 750 \text{ MeV}/c$. Candidate $\mu^+\mu^-\pi^+\pi^-$ combinations that form a good quality common vertex are retained, and the tracks are refit with kinematic constraints that fix the $\mu^+\mu^-$ invariant mass to the known J/ψ mass and require all four tracks to have the same origin point [43].

Simulation is required to model the effects of the detector acceptance and the selection requirements. In the simulation, pp collisions are generated using PYTHIA [44] with a specific LHCb configuration [45]. Decays of unstable particles are described by EVTGEN [46]. The interaction of the generated particles with the detector and its response are implemented using the GEANT4 toolkit [47] as described in Ref. [48]. The p_T distributions of the simulated B_s^0 and B^0 mesons, the invariant mass distributions of $\pi^+\pi^-$ pairs from their decays, and simulated event multiplicity distributions are weighted to match background-subtracted distributions that are extracted from the data using the *sPlot* method [49].

The multiplicity metrics used in this analysis are the total number of charged tracks reconstructed in the VELO detector, $N_{\text{tracks}}^{\text{VELO}}$, and the subset of VELO tracks that point in the backward direction, away from the LHCb spectrometer, $N_{\text{tracks}}^{\text{back}}$. The backward tracks cover a pseudorapidity interval of approximately $-3.5 < \eta < -1.5$, providing a multiplicity estimate that is measured in a different region

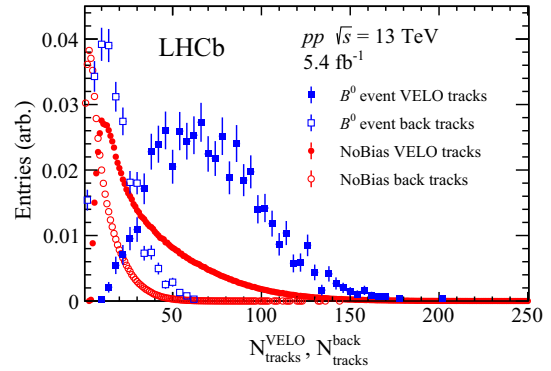


FIG. 1. Distribution of the number of VELO tracks and backward tracks for NoBias events (red) and B^0 signal events (blue), each with only one primary vertex. The vertical scale is arbitrary.

than the signal. The VELO detector and its performance are described in detail in Refs. [39,40]. Figure 1 shows the distributions of $N_{\text{tracks}}^{\text{VELO}}$ and $N_{\text{tracks}}^{\text{back}}$ for both NoBias events and B^0 signal events with one reconstructed primary vertex, which requires at least five reconstructed tracks. NoBias events are selected based on the Large Hadron Collider beam clock, which indicates that a bunch crossing has occurred, without any other trigger requirements. The distributions for B^0 signal events are extracted from the data, and background is removed using the *sPlot* method [49]. The results are quoted in terms of normalized multiplicity, defined as the number of tracks at the center of a given multiplicity interval divided by the mean number of tracks in NoBias events, which are $\langle N_{\text{tracks}}^{\text{VELO}} \rangle_{\text{NoBias}} = 37.7$ and $\langle N_{\text{tracks}}^{\text{back}} \rangle_{\text{NoBias}} = 11.1$, with negligibly small uncertainties. For comparison, the mean number of $N_{\text{tracks}}^{\text{VELO}}$ and $N_{\text{tracks}}^{\text{back}}$ are 71.1 ± 0.1 and 17.4 ± 0.3 for B^0 signal events, respectively, where the uncertainty is due to the statistical uncertainty on the track distributions. In some respects, the low- and high-multiplicity data samples approach the hadronic environments achieved in e^+e^- collisions and heavy-ion collisions, respectively.

The sample containing signal events is divided into intervals of multiplicity, and in each interval a likelihood fit is performed on the $J/\psi\pi^+\pi^-$ invariant mass spectrum to determine the ratio of B_s^0 to B^0 yields. Examples of the $J/\psi\pi^+\pi^-$ mass distribution in low- and high-multiplicity intervals are shown in Fig. 2. An increase of the B_s^0 yield relative to the B^0 yield in the high-multiplicity interval is apparent. The B_s^0 and B^0 peaks are each represented in the fit by a sum of two Crystal Ball functions, which have tail parameters constrained to values determined by simulation. The background contribution is represented by an exponential function, which is found to provide a good description of the purely combinatorial $J/\psi\pi^+\pi^\pm$ mass spectrum with like-sign dipions. All multiplicity intervals are fit simultaneously, where the signal shapes are constrained to be the same in each interval, but their

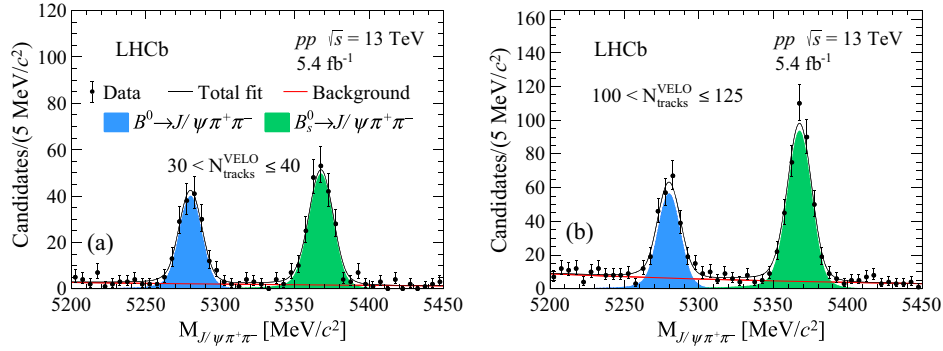


FIG. 2. Measured $J/\psi\pi^+\pi^-$ invariant mass distributions and fit projections in the multiplicity ranges (a) $30 < N_{\text{tracks}}^{\text{VELO}} \leq 40$ and (b) $100 < N_{\text{tracks}}^{\text{VELO}} \leq 125$.

normalization and the background parameters are allowed to vary. The B_s^0 and B^0 line shapes are nearly identical, and variations of the fit functions have a negligible effect on the extracted ratio of B_s^0 to B^0 yields.

The ratio of cross sections $\sigma_{B_s^0}/\sigma_{B^0}$ is found by calculating

$$\frac{\sigma_{B_s^0}}{\sigma_{B^0}} = \frac{N_{B_s^0}}{N_{B^0}} \times \frac{\mathcal{B}_{B^0}}{\mathcal{B}_{B_s^0}} \times \frac{\epsilon_{B^0}^{\text{acc}}}{\epsilon_{B_s^0}^{\text{acc}}} \times \frac{\epsilon_{B^0}^{\text{trig}}}{\epsilon_{B_s^0}^{\text{trig}}} \times \frac{\epsilon_{B^0}^{\text{PID}}}{\epsilon_{B_s^0}^{\text{PID}}} \times \frac{\epsilon_{B^0}^{\text{reco}}}{\epsilon_{B_s^0}^{\text{reco}}}, \quad (1)$$

where $N_{B_s^0}/N_{B^0}$ is the ratio of B_s^0 to B^0 signal yields returned by the fit, $\mathcal{B}_{B^0}/\mathcal{B}_{B_s^0}$ is the ratio of B^0 to B_s^0 branching fractions to $J/\psi\pi^+\pi^-$ [19,50], and $\epsilon_{B^0}^{\text{acc}}/\epsilon_{B_s^0}^{\text{acc}}$, $\epsilon_{B^0}^{\text{trig}}/\epsilon_{B_s^0}^{\text{trig}}$, $\epsilon_{B^0}^{\text{PID}}/\epsilon_{B_s^0}^{\text{PID}}$, and $\epsilon_{B^0}^{\text{reco}}/\epsilon_{B_s^0}^{\text{reco}}$ are ratios of the LHCb acceptance and the trigger, particle identification, and reconstruction efficiencies for B^0 to B_s^0 mesons, respectively. Because of the similarities of the B_s^0 and B^0 decays, many systematic uncertainties partially cancel in this ratio of cross sections. The ratio of the LHCb acceptance for the decays $\epsilon_{B^0}^{\text{acc}}/\epsilon_{B_s^0}^{\text{acc}}$ is found, using simulation, to be consistent with unity, with an uncertainty of $\sim 1\%$ due to the uncertainty on the weights applied to the simulation in order to match the data. The ratio of trigger efficiencies $\epsilon_{B^0}^{\text{trig}}/\epsilon_{B_s^0}^{\text{trig}}$ is determined from data to be consistent with unity, with an uncertainty of $\sim 1\%$, using techniques described in Ref. [51], where the uncertainty comes from statistical uncertainties on the data sample. The ratio of particle identification efficiencies $\epsilon_{B^0}^{\text{PID}}/\epsilon_{B_s^0}^{\text{PID}}$ is found using calibrated samples of identified muons and pions obtained from the data and is consistent with unity with an uncertainty of $\sim 1\%$ due to the finite size of the calibration sample. The only term with a significant difference from unity is the ratio of reconstruction efficiencies, which is found to be $\epsilon_{B^0}^{\text{reco}}/\epsilon_{B_s^0}^{\text{reco}} = 0.86 \pm 0.04$ for the p_T -integrated sample. This is due to the difference in the dipion mass distributions produced in the B_s^0 and B^0 decays: The B_s^0 decay is dominated by contributions from intermediate

$f_0(980)$ and $f_0(1500)$ states [52], which are reconstructed with higher efficiency than the lower-mass $\rho^0(770)$ intermediate state that is significant in B^0 decays [53]. The uncertainty on this correction is due to the statistical uncertainty on the weights extracted from the data that are applied to the simulation in order to match the measured B meson p_T and dipion mass distributions.

The ratio of cross sections for the multiplicity-integrated samples is found to be $\sigma_{B_s^0}/\sigma_{B^0} = 0.30 \pm 0.01 \pm 0.03$, where the first uncertainty is statistical and the second is systematic. This measurement agrees with previous LHCb measurements of f_s/f_d using different decay channels [19] within 1.5 standard deviations.

The multiplicity dependence of $\sigma_{B_s^0}/\sigma_{B^0}$ is shown in Fig. 3, for two different multiplicity metrics. The vertical error bars (boxes) represent point-to-point uncorrelated (fully correlated) uncertainties, while the horizontal error bars represent the bin width. Numerical values are given in Supplemental Material [54]. In the left panel, the ratio shows an increasing trend with the total VELO multiplicity, where multiplicity is normalized to the mean value found in

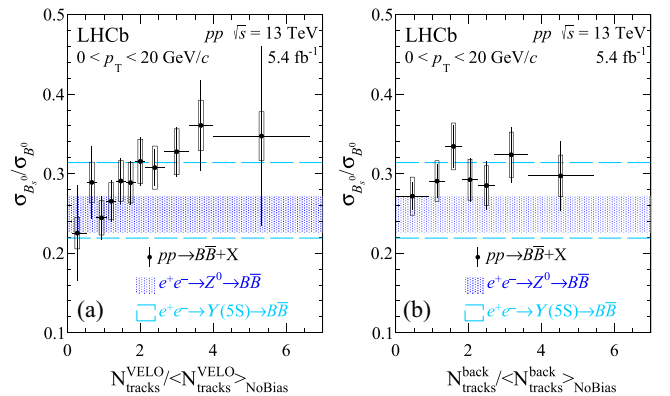


FIG. 3. Ratio of cross sections $\sigma_{B_s^0}/\sigma_{B^0}$ versus the normalized multiplicity of (a) all VELO tracks and (b) backward VELO tracks. The vertical error bars (boxes) represent point-to-point uncorrelated (fully correlated) uncertainties. The horizontal bands show the values measured in e^+e^- collisions.

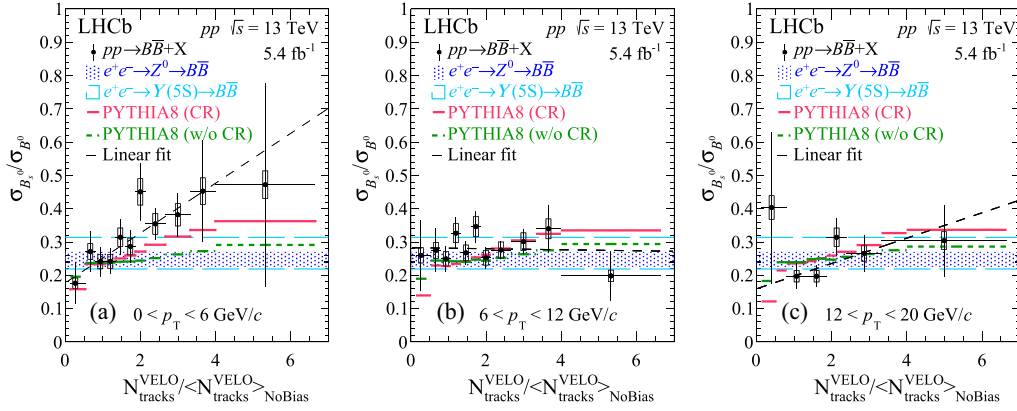


FIG. 4. Ratio of cross sections $\sigma_{B_s^0}/\sigma_{B^0}$ versus normalized multiplicity in the transverse momentum ranges (a) $0 < p_T < 6$ GeV/c, (b) $6 < p_T < 12$ GeV/c, and (c) $12 < p_T < 20$ GeV/c. The vertical error bars (boxes) represent point-to-point uncorrelated (fully correlated) uncertainties. The horizontal bands show the values measured in e^+e^- collisions, and the horizontal lines show PYTHIA calculations with and without (w/o) color reconnection.

NoBias collisions. Also shown are the $\sigma_{B_s^0}/\sigma_{B^0}$ values measured in e^+e^- collisions at the $\Upsilon(5S)$ and Z^0 resonances [55], which are in good agreement with the data at low multiplicity. The right panel shows the same ratio versus the normalized $N_{\text{tracks}}^{\text{back}}$. No significant dependence is observed on the multiplicity measured in the backward region. The dependence on total multiplicity, compared to the lack of dependence on multiplicity measured at backward rapidity, could indicate that the mechanism responsible for the increase in the $\sigma_{B_s^0}/\sigma_{B^0}$ ratio is related to the local particle density in a similar rapidity interval as the B mesons themselves.

The multiplicity dependence of $\sigma_{B_s^0}/\sigma_{B^0}$ is shown in three different intervals of B meson p_T in Fig. 4. Numerical values are given in Supplemental Material [54]. The lowest p_T interval, $0 < p_T < 6$ GeV/c, encompasses B mesons with p_T approximately equal to or less than their mass. In this p_T interval, at low multiplicity the $\sigma_{B_s^0}/\sigma_{B^0}$ ratio is consistent with values measured in e^+e^- collisions and increases with multiplicity. A line fit to these data returns a slope of $0.075 \pm 0.022 (N_{\text{tracks}}^{\text{VELO}}/\langle N_{\text{tracks}}^{\text{VELO}} \rangle_{\text{NoBias}})^{-1}$, which differs from zero by 3.4 standard deviations and thereby provides evidence for an increase of the $\sigma_{B_s^0}/\sigma_{B^0}$ ratio. This fit considers only the point-to-point uncorrelated uncertainties; since all data points must move simultaneously within the correlated uncertainties, they have no effect on the extracted slope.

For comparison, the ratio of cross sections calculated by the PYTHIA event generator is also shown. Events are generated with and without color reconnection (CR), a process which allows partons produced by different interactions in the collision to be connected by color lines [56,57]. Color reconnection was introduced to model charged particle production in hadron collisions and is thought to be especially important in high-multiplicity collisions where multiple-parton interactions are significant.

Both sets of PYTHIA calculations show a rise with multiplicity, which is more pronounced when CR is included. The PYTHIA models agree with the data at relatively low multiplicity, but both scenarios give values that are lower than the central values of the data at high multiplicity.

The measurements in higher p_T intervals, $6 < p_T < 12$ GeV/c and $12 < p_T < 20$ GeV/c, display no significant dependence on multiplicity and are consistent with data from e^+e^- collisions. This behavior is expected in a scenario where low- p_T b quarks with relatively low velocity recombine with s quarks produced in high-multiplicity collisions, while the wave functions of higher- p_T b quarks have less overlap with the low- p_T bulk of the quarks produced in the collision. These high- p_T b quarks would thereby dominantly hadronize via fragmentation in vacuum, as in e^+e^- collisions, rather than via coalescence. Again, both sets of PYTHIA calculations show a rising trend, which is more pronounced when color reconnection is included. However, here the uncertainties on the data prevent discrimination between the two scenarios. Lines fit to the $6 < p_T < 12$ GeV/c and $12 < p_T < 20$ GeV/c data have slopes that are consistent with zero within 0.2 and 1.3 standard deviations, respectively.

In summary, LHCb measurements in pp collisions at $\sqrt{s} = 13$ TeV show evidence that the production of B_s^0 mesons is enhanced relative to B^0 mesons in collisions with high charged-particle multiplicity, indicating that strangeness enhancement is present in B hadron production. In collisions with relatively low charged-particle multiplicity, and for B mesons with $p_T > 6$ GeV/c, the rate of B_s^0 production relative to B^0 production is consistent with what is measured in e^+e^- collisions. These measurements are qualitatively consistent with expectations based on the emergence of quark coalescence as an additional hadronization mechanism rather than fragmentation alone. These results could indicate that interactions of the b quarks with

the local hadronic environment influence the hadronization process, thereby breaking factorization of b quark hadronization between e^+e^- and hadron collisions.

We express our gratitude to our colleagues in the CERN accelerator departments for the excellent performance of the LHC. We thank the technical and administrative staff at the LHCb institutes. We acknowledge support from CERN and from the national agencies: CAPES, CNPq, FAPERJ, and FINEP (Brazil); MOST and NSFC (China); CNRS/IN2P3 (France); BMBF, DFG, and MPG (Germany); INFN (Italy); NWO (Netherlands); MNiSW and NCN (Poland); MEN/IFA (Romania); MICINN (Spain); SNSF and SER (Switzerland); NASU (Ukraine); STFC (United Kingdom); DOE NP and NSF (USA). We acknowledge the computing resources that are provided by CERN, IN2P3 (France), KIT and DESY (Germany), INFN (Italy), SURF (Netherlands), PIC (Spain), GridPP (United Kingdom), CSCS (Switzerland), IFIN-HH (Romania), CBPF (Brazil), Polish WLCG (Poland), and NERSC (USA). We are indebted to the communities behind the multiple open-source software packages on which we depend. Individual groups or members have received support from ARC and ARDC (Australia); Minciencias (Colombia); AvH Foundation (Germany); EPLANET, Marie Skłodowska-Curie Actions, and ERC (European Union); A*MIDEX, ANR, IPhU and Labex P2IO, and Région Auvergne-Rhône-Alpes (France); Key Research Program of Frontier Sciences of CAS, CAS PIFI, CAS CCEPP, Fundamental Research Funds for the Central Universities, and Sci. and Tech. Program of Guangzhou (China); GVA, XuntaGal, GENCAT, and Prog. Atracción Talento, CM (Spain); SRC (Sweden); the Leverhulme Trust, the Royal Society, and UKRI (United Kingdom).

[1] E. Norrbin and T. Sjostrand, Production and hadronization of heavy quarks, *Eur. Phys. J. C* **17**, 137 (2000).
 [2] R. Aaij *et al.* (LHCb Collaboration), Measurement of the b -Quark Production Cross-Section in 7 and 13 TeV pp Collisions, *Phys. Rev. Lett.* **118**, 052002 (2017); **119**, 169901(E) (2017).
 [3] R. Aaij *et al.* (LHCb Collaboration), Measurement of the B^\pm production cross-section in $p p$ collisions at $\sqrt{s} = 7$ and 13 TeV, *J. High Energy Phys.* **12** (2017) 026,
 [4] S. Acharya *et al.* (ALICE Collaboration), Measurement of beauty and charm production in pp collisions at $\sqrt{s} = 5.02$ TeV via non-prompt and prompt D mesons, *J. High Energy Phys.* **05** (2021) 220.
 [5] B. Andersson, G. Gustafson, G. Ingelman, and T. Sjostrand, Parton fragmentation and string dynamics, *Phys. Rep.* **97**, 31 (1983).
 [6] B. R. Webber, A QCD model for jet fragmentation including soft gluon interference, *Nucl. Phys.* **B238**, 492 (1984).
 [7] M. Artuso *et al.* (CLEO Collaboration), First Evidence and Measurement of $B_s^{(*)}\bar{B}_s^{(*)}$ Production at the $\Upsilon(5S)$, *Phys. Rev. Lett.* **95**, 261801 (2005).

[8] A. Drutskoy *et al.* (Belle Collaboration), Measurement of Inclusive D_s, D^0 and J/ψ Rates and Determination of the $B_s^{(*)}\bar{B}_s^{(*)}$ Production Fraction in $b\bar{b}$ Events at the $\Upsilon(5S)$ Resonance, *Phys. Rev. Lett.* **98**, 052001 (2007).
 [9] G. S. Huang *et al.* (CLEO Collaboration), Measurement of $B(\Upsilon(5S) \rightarrow B_s^{(*)}\bar{B}_s^{(*)})$ using ϕ mesons, *Phys. Rev. D* **75**, 012002 (2007).
 [10] P. D. Acton *et al.* (OPAL Collaboration), Evidence for the existence of the strange b flavored meson B_s^0 in Z^0 decays, *Phys. Lett. B* **295**, 357 (1992).
 [11] D. Buskulic *et al.* (ALEPH Collaboration), Measurement of the B_s^0 lifetime and production rate with $D_s - \ell^+$ combinations in Z decays, *Phys. Lett. B* **361**, 221 (1995).
 [12] M. Acciarri *et al.* (L3 Collaboration), Measurements of the $b\bar{b}$ production cross-section and forward backward asymmetry at center-of-mass energies above the Z pole at LEP, *Phys. Lett. B* **485**, 71 (2000).
 [13] J. Abdallah *et al.* (DELPHI Collaboration), A measurement of the branching fractions of the b quark into charged and neutral b hadrons, *Phys. Lett. B* **576**, 29 (2003).
 [14] J. C. Collins, D. E. Soper, and G. Sterman, Factorization of hard processes in QCD, *Adv. Ser. Dir. High Energy Phys.* **5**, 1 (1989).
 [15] F. Abe *et al.* (CDF Collaboration), Ratios of bottom meson branching fractions involving J/ψ mesons and determination of b quark fragmentation fractions, *Phys. Rev. D* **54**, 6596 (1996).
 [16] R. Aaij *et al.* (LHCb Collaboration), Measurement of the fragmentation fraction ratio f_s/f_d and its dependence on B meson kinematics, *J. High Energy Phys.* **04** (2013) 001.
 [17] G. Aad *et al.* (ATLAS Collaboration), Determination of the Ratio of b -Quark Fragmentation Fractions f_s/f_d in pp Collisions at $\sqrt{s} = 7$ TeV with the ATLAS Detector, *Phys. Rev. Lett.* **115**, 262001 (2015).
 [18] R. Aaij *et al.* (LHCb Collaboration), Measurement of f_s/f_u Variation with Proton-Proton Collision Energy and B -Meson Kinematics, *Phys. Rev. Lett.* **124**, 122002 (2020).
 [19] R. Aaij *et al.* (LHCb Collaboration), Precise measurement of the f_s/f_d ratio of fragmentation fractions and of B_s^0 decay branching fractions, *Phys. Rev. D* **104**, 032005 (2021).
 [20] R. Aaij *et al.* (LHCb Collaboration), Measurement of b hadron production fractions in 7 TeV $p p$ collisions, *Phys. Rev. D* **85**, 032008 (2012).
 [21] R. Aaij *et al.* (LHCb Collaboration), Measurement of b -hadron fractions in 13 TeV $p p$ collisions, *Phys. Rev. D* **100**, 031102(R) (2019).
 [22] S. Acharya *et al.* (ALICE Collaboration), Charm-quark fragmentation fractions and production cross section at midrapidity in pp collisions at the LHC, *Phys. Rev. D* **105**, L011103 (2022).
 [23] A. V. Berezhnoy and A. K. Likhoded, Relative yield of heavy hadrons as a function of the transverse momentum in LHC experiments, *Phys. At. Nucl.* **78**, 292 (2015).
 [24] R. Vogt and S. J. Brodsky, QCD and intrinsic heavy quark predictions for leading charm and beauty hadroproduction, *Nucl. Phys.* **B438**, 261 (1995).
 [25] E. Braaten, Y. Jia, and T. Mehen, The Leading Particle Effect from Heavy Quark Recombination, *Phys. Rev. Lett.* **89**, 122002 (2002).

- [26] R. Rapp and E. V. Shuryak, D meson production from recombination in hadronic collisions, *Phys. Rev. D* **67**, 074036 (2003).
- [27] M. He and R. Rapp, Hadronization and Charm-Hadron Ratios in Heavy-Ion Collisions, *Phys. Rev. Lett.* **124**, 042301 (2020).
- [28] V. Minissale, S. Plumari, and V. Greco, Charm hadrons in pp collisions at LHC energy within a coalescence plus fragmentation approach, *Phys. Lett. B* **821**, 136622 (2021).
- [29] R. J. Fries, B. Muller, C. Nonaka, and S. A. Bass, Hadronization in Heavy Ion Collisions: Recombination and Fragmentation of Partons, *Phys. Rev. Lett.* **90**, 202303 (2003).
- [30] V. Greco, C. M. Ko, and P. Levai, Parton Coalescence and Anti-Proton / Pion Anomaly at RHIC, *Phys. Rev. Lett.* **90**, 202302 (2003).
- [31] D. Molnar and S. A. Voloshin, Elliptic Flow at Large Transverse Momenta from Quark Coalescence, *Phys. Rev. Lett.* **91**, 092301 (2003).
- [32] A. M. Sirunyan *et al.* (CMS Collaboration), Measurement of B_s^0 meson production in pp and PbPb collisions at $\sqrt{s_{NN}} = 5.02$ TeV, *Phys. Lett. B* **796**, 168 (2019).
- [33] A. Tumasyan *et al.* (CMS Collaboration), Observation of B_s^0 mesons and measurement of the B_s^0/B^+ yield ratio in PbPb collisions at $\sqrt{s_{NN}} = 5.02$ TeV, *Phys. Lett. B* **829**, 137062 (2022).
- [34] V. Khachatryan *et al.* (CMS Collaboration), Observation of long-range near-side angular correlations in proton-proton collisions at the LHC, *J. High Energy Phys.* **09** (2010) 091.
- [35] G. Aad *et al.* (ATLAS Collaboration), Observation of Long-Range Elliptic Azimuthal Anisotropies in $\sqrt{s} = 13$ and 2.76 TeV pp Collisions with the ATLAS Detector, *Phys. Rev. Lett.* **116**, 172301 (2016).
- [36] V. Khachatryan *et al.* (CMS Collaboration), Evidence for collectivity in pp collisions at the LHC, *Phys. Lett.* **65B**, 193 (2017).
- [37] J. Adam *et al.* (ALICE Collaboration), Enhanced production of multi-strange hadrons in high-multiplicity proton-proton collisions, *Nat. Phys.* **13**, 535 (2017).
- [38] P. Koch, B. Muller, and J. Rafelski, Strangeness in relativistic heavy ion collisions, *Phys. Rep.* **142**, 167 (1986).
- [39] LHCb Collaboration, LHCb VELO (Vertex LOcator): Technical Design Report, Report No. CERN-LHCC-2001-011, CERN, Geneva, 2001.
- [40] R. Aaij *et al.*, Performance of the LHCb vertex locator, *J. Instrum.* **9**, P09007 (2014).
- [41] A. A. Alves Jr. *et al.* (LHCb Collaboration), The LHCb detector at the LHC, *J. Instrum.* **3**, S08005 (2008).
- [42] R. Aaij *et al.* (LHCb Collaboration), LHCb detector performance, *Int. J. Mod. Phys. A* **30**, 1530022 (2015).
- [43] W. D. Hulsbergen, Decay chain fitting with a Kalman filter, *Nucl. Instrum. Methods Phys. Res., Sect. A* **552**, 566 (2005).
- [44] T. Sjöstrand, S. Mrenna, and P. Skands, A brief introduction to PYTHIA8.1, *Comput. Phys. Commun.* **178**, 852 (2008); PYTHIA6.4 physics and manual, *J. High Energy Phys.* **05** (2006) 026.
- [45] I. Belyaev *et al.*, Handling of the generation of primary events in Gauss, the LHCb simulation framework, *J. Phys. Conf. Ser.* **331**, 032047 (2011).
- [46] D. J. Lange, The EVTGEN particle decay simulation package, *Nucl. Instrum. Methods Phys. Res., Sect. A* **462**, 152 (2001).
- [47] J. Allison *et al.* (GEANT4 Collaboration), GEANT4 developments and applications, *IEEE Trans. Nucl. Sci.* **53**, 270 (2006); S. Agostinelli *et al.* (GEANT4 Collaboration), GEANT4: A simulation toolkit, *Nucl. Instrum. Methods Phys. Res., Sect. A* **506**, 250 (2003).
- [48] M. Clemencic, G. Corti, S. Easo, C. R. Jones, S. Miglioranza, M. Pappagallo, and P. Robbe, The LHCb simulation application, Gauss: Design, evolution and experience, *J. Phys. Conf. Ser.* **331**, 032023 (2011).
- [49] M. Pivk and F. R. Le Diberder, SPlot: A statistical tool to unfold data distributions, *Nucl. Instrum. Methods Phys. Res., Sect. A* **555**, 356 (2005).
- [50] P. A. Zyla *et al.* (Particle Data Group), Review of particle physics, *Prog. Theor. Exp. Phys.* **2020**, 083C01 (2020).
- [51] S. Tolck, J. Albrecht, F. Dettori, and A. Pellegrino, Data driven trigger efficiency determination at LHCb, Report No. LHCb-PUB-2014-039, CERN, Geneva, 2014.
- [52] R. Aaij *et al.* (LHCb Collaboration), Measurement of resonant and CP components in $\bar{B}_s^0 \rightarrow J/\psi\pi^+\pi^-$ decays, *Phys. Rev. D* **89**, 092006 (2014).
- [53] R. Aaij *et al.* (LHCb Collaboration), Measurement of the resonant and CP components in $\bar{B}^0 \rightarrow J/\psi\pi^+\pi^-$ decays, *Phys. Rev. D* **90**, 012003 (2014).
- [54] See Supplemental Material at <http://link.aps.org/supplemental/10.1103/PhysRevLett.131.061901> for numerical values of cross section ratios.
- [55] Y. S. Amhis *et al.* (HFLAV Collaboration), Averages of b-hadron, c-hadron, and τ -lepton properties as of 2018, *Eur. Phys. J. C* **81**, 226 (2021).
- [56] T. Sjostrand and M. van Zijl, A multiple interaction model for the event structure in hadron collisions, *Phys. Rev. D* **36**, 2019 (1987).
- [57] T. Sjöstrand, Colour reconnection and its effects on precise measurements at the LHC, [arXiv:1310.8073](https://arxiv.org/abs/1310.8073).

R. Aaij^{1,2,32}, A. S. W. Abdelmotteleb^{1,50}, C. Abellan Beteta⁴⁴, F. Abudinén⁵⁰, T. Ackernley⁵⁴, B. Adeva⁴⁰, M. Adinolfi⁴⁸, H. Afsharnia⁹, C. Agapopoulou¹³, C. A. Aidala⁷⁶, S. Aiola²⁵, Z. Ajaltouni⁹, S. Akar⁵⁹, K. Akiba³², J. Albrecht¹⁵, F. Alessio⁴², M. Alexander⁵³, A. Alfonso Albergo³⁹, Z. Aliouche⁵⁶, P. Alvarez Cartelle⁴⁹, S. Amato², J. L. Amey⁴⁸, Y. Amhis^{11,42}, L. An⁴², L. Anderlini²², M. Andersson⁴⁴, A. Andreianov³⁸, M. Andreotti²¹, D. Andreou⁶², D. Ao⁶, F. Archilli¹⁷, A. Artamonov³⁸, M. Artuso⁶², E. Aslanides¹⁰, M. Atzeni⁴⁴, B. Audurier¹², S. Bachmann¹⁷, M. Bachmayer⁴³, J. J. Back⁵⁰, A. Bailly-reyre¹³

P. Baladron Rodriguez⁴⁰, V. Balagura¹², W. Baldini²¹, J. Baptista de Souza Leite¹, M. Barbetti^{22,b}, R. J. Barlow⁵⁶, S. Barsuk¹¹, W. Barter⁵⁵, M. Bartolini⁴⁹, F. Baryshnikov³⁸, J. M. Basels¹⁴, G. Bassi^{29,c}, B. Batsukh⁴, A. Battig¹⁵, A. Bay⁴³, A. Beck⁵⁰, M. Becker¹⁵, F. Bedeschi²⁹, I. B. Bediaga¹, A. Beiter⁶², V. Belavin³⁸, S. Belin⁴⁰, V. Bellee⁴⁴, K. Belous³⁸, I. Belov³⁸, I. Belyaev³⁸, G. Bencivenni²³, E. Ben-Haim¹³, A. Berezhnoy³⁸, R. Bernet⁴⁴, D. Berninghoff¹⁷, H. C. Bernstein⁶², C. Bertella⁵⁶, A. Bertolin²⁸, C. Betancourt⁴⁴, F. Betti⁴², Ia. Bezshyiko⁴⁴, S. Bhasin⁴⁸, J. Bhom³⁵, L. Bian⁶⁷, M. S. Bieker¹⁵, N. V. Biesuz²¹, S. Bifani⁴⁷, P. Billoir¹³, A. Biolchini³², M. Birch⁵⁵, F. C. R. Bishop⁴⁹, A. Bitadze⁵⁶, A. Bizzeti⁶, M. Bjørn⁵⁷, M. P. Blago⁴⁹, T. Blake⁵⁰, F. Blanc⁴³, S. Blusk⁶², D. Bobulska⁵³, J. A. Boelhauve¹⁵, O. Boente Garcia⁴⁰, T. Boettcher⁵⁹, A. Boldyrev³⁸, N. Bondar^{38,42}, S. Borghi⁵⁶, M. Borsato¹⁷, J. T. Borsuk³⁵, S. A. Bouchiba⁴³, T. J. V. Bowcock^{54,42}, A. Boyer⁴², C. Bozzi²¹, M. J. Bradley⁵⁵, S. Braun⁶⁰, A. Brea Rodriguez⁴⁰, J. Brodzicka³⁵, A. Brossa Gonzalo⁵⁰, D. Brundu²⁷, A. Buonauro⁴⁴, L. Buonincontri²⁸, A. T. Burke⁵⁶, C. Burr⁴², A. Bursche⁶⁶, A. Butkevich³⁸, J. S. Butter³², J. Buytaert⁴², W. Byczynski⁴², S. Cadeddu²⁷, H. Cai⁶⁷, R. Calabrese^{21,d}, L. Calefice^{15,13}, S. Cali²³, R. Calladine⁴⁷, M. Calvi^{26,e}, M. Calvo Gomez⁷⁴, P. Camargo Magalhaes⁴⁸, P. Campana²³, D. H. Campora Perez⁷³, A. F. Campoverde Quezada⁶, S. Capelli^{26,e}, L. Capriotti^{20,f}, A. Carbone^{20,f}, G. Carboni³¹, R. Cardinale^{24,g}, A. Cardini²⁷, I. Carli⁴, P. Carniti^{26,e}, L. Carus¹⁴, A. Casais Vidal⁴⁰, R. Caspary¹⁷, G. Casse⁵⁴, M. Cattaneo⁴², G. Cavallero⁴², V. Cavallini^{21,d}, S. Celani⁴³, J. Cerasoli¹⁰, D. Cervenkov⁵⁷, A. J. Chadwick⁵⁴, M. G. Chapman⁴⁸, M. Charles¹³, Ph. Charpentier⁴², C. A. Chavez Barajas⁵⁴, M. Chefdeville⁸, C. Chen³, S. Chen⁴, A. Chernov³⁵, S. Chernyshenko⁴⁶, V. Chobanova⁴⁰, S. Cholak⁴³, M. Chrzaszcz³⁵, A. Chubykin³⁸, V. Chulikov³⁸, P. Ciambrone²³, M. F. Cicala⁵⁰, X. Cid Vidal⁴⁰, G. Ciezarek⁴², G. Ciullo^{21,d}, P. E. L. Clarke⁵², M. Clemencic⁴², H. V. Cliff⁴⁹, J. Closier⁴², J. L. Cobbledick⁵⁶, V. Coco⁴², J. A. B. Coelho¹¹, J. Cogan¹⁰, E. Cogneras⁹, L. Cojocariu³⁷, P. Collins⁴², T. Colombo⁴², L. Congedo^{19,h}, A. Contu²⁷, N. Cooke⁴⁷, G. Coombs⁵³, I. Corredoira⁴⁰, G. Corti⁴², B. Couturier⁴², D. C. Craik⁵⁸, J. Crkovská⁶¹, M. Cruz Torres^{1,i}, R. Currie⁵², C. L. Da Silva⁶¹, S. Dadabaev³⁸, L. Dai⁶⁵, E. Dall'Occo¹⁵, J. Dalseno⁴⁰, C. D'Ambrosio⁴², A. Danilina³⁸, P. d'Argent¹⁵, J. E. Davies⁵⁶, A. Davis⁵⁶, O. De Aguiar Francisco⁵⁶, J. de Boer⁴², K. De Bruyn⁷², S. De Capua⁵⁶, M. De Cian⁴³, U. De Freitas Carneiro Da Graca¹, E. De Lucia²³, J. M. De Miranda¹, L. De Paula², M. De Serio^{19,h}, D. De Simone⁴⁴, P. De Simone²³, F. De Vellis¹⁵, J. A. de Vries⁷³, C. T. Dean⁶¹, F. Debernardis^{19,h}, D. Decamp⁸, V. Dedu¹⁰, L. Del Buono¹³, B. Delaney⁴⁹, H.-P. Dembinski¹⁵, V. Denysenko⁴⁴, O. Deschamps⁹, F. Dettori^{27,j}, B. Dey⁷⁰, A. Di Cicco²³, P. Di Nezza²³, S. Didenko³⁸, L. Dieste Maronas⁴⁰, S. Ding⁶², V. Dobishuk⁴⁶, A. Dolmatov³⁸, C. Dong³, A. M. Donohoe¹⁸, F. Dordei²⁷, A. C. dos Reis¹, L. Douglas⁵³, A. G. Downes⁸, M. W. Dudek³⁵, L. Dufour⁴², V. Duk⁷¹, P. Durante⁴², J. M. Durham⁶¹, D. Dutta⁵⁶, A. Dziurda³⁵, A. Dzyuba³⁸, S. Easo⁵¹, U. Egede⁶³, V. Egorychev³⁸, S. Eidelman^{38,a}, S. Eisenhardt⁵², S. Ek-In⁴³, L. Eklund⁷⁵, S. Ely⁶², A. Ene³⁷, E. Epple⁶¹, S. Escher¹⁴, J. Eschle⁴⁴, S. Esen⁴⁴, T. Evans⁵⁶, L. N. Falcao¹, Y. Fan⁶, B. Fang⁶⁷, S. Farry⁵⁴, D. Fazzini^{26,e}, M. Feo⁴², A. D. Ferez⁶⁰, F. Ferrari²⁰, L. Ferreira Lopes⁴³, F. Ferreira Rodrigues², S. Ferreres Sole³², M. Ferrillo⁴⁴, M. Ferro-Luzzi⁴², S. Filippov³⁸, R. A. Fini¹⁹, M. Fiorini^{21,d}, M. Firlej³⁴, K. M. Fischer⁵⁷, D. S. Fitzgerald⁷⁶, C. Fitzpatrick⁵⁶, T. Fiutowski³⁴, F. Fleuret¹², M. Fontana¹³, F. Fontanelli^{24,g}, R. Forty⁴², D. Foulds-Holt⁴⁹, V. Franco Lima⁵⁴, M. Franco Sevilla⁶⁰, M. Frank⁴², E. Franzoso^{21,d}, G. Frau¹⁷, C. Frei⁴², D. A. Friday⁵³, J. Fu⁶, Q. Fuehring¹⁵, E. Gabriel³², G. Galati^{19,h}, A. Gallas Torreira⁴⁰, D. Galli^{20,f}, S. Gambetta^{52,42}, Y. Gan³, M. Gandelman², P. Gandini²⁵, Y. Gao⁵, M. Garau^{27,j}, L. M. Garcia Martin⁵⁰, P. Garcia Moreno³⁹, J. García Pardiñas^{26,e}, B. Garcia Plana⁴⁰, F. A. Garcia Rosales¹², L. Garrido³⁹, C. Gaspar⁴², R. E. Geertsema³², D. Gerick¹⁷, L. L. Gerken¹⁵, E. Gersabeck⁵⁶, M. Gersabeck⁵⁶, T. Gershon⁵⁰, L. Giambastiani²⁸, V. Gibson⁴⁹, H. K. Gienza³⁶, A. L. Gilman⁵⁷, M. Giovannetti^{23,k}, A. Gioventù⁴⁰, P. Gironella Gironell³⁹, C. Giugliano^{21,d}, K. Gizdov⁵², E. L. Gkougkousis⁴², V. V. Gligorov^{13,42}, C. Göbel⁶⁴, E. Golobardes⁷⁴, D. Golubkov³⁸, A. Golutvin^{55,38}, A. Gomes^{1,2,a,l}, S. Gomez Fernandez³⁹, F. Goncalves Abrantes⁵⁷, M. Goncerz³⁵, G. Gong³, I. V. Gorelov³⁸, C. Gotti²⁶, J. P. Grabowski¹⁷, T. Grammatico¹³, L. A. Granado Cardoso⁴², E. Graugés³⁹, E. Graverini⁴³, G. Graziani⁶, A. T. Grecu³⁷, L. M. Greeven³², N. A. Grieser⁴, L. Grillo⁵³, S. Gromov³⁸, B. R. Gruberg Cazon⁵⁷, C. Gu³, M. Guarise^{21,d}, M. Guittiere¹¹, P. A. Günther¹⁷, E. Gushchin³⁸, A. Guth¹⁴, Y. Guz³⁸, T. Gys⁴², T. Hadavizadeh⁶³, G. Haefeli⁴³, C. Haen⁴², J. Haimberger⁴², S. C. Haines⁴⁹, T. Halewood-leagas⁵⁴, M. M. Halvorsen⁴², P. M. Hamilton⁶⁰

J. Hammerich⁵⁴, Q. Han⁷, X. Han¹⁷, E. B. Hansen⁵⁶, S. Hansmann-Menzemer^{17,42}, L. Hao⁶, N. Harnew⁵⁷, T. Harrison⁵⁴, C. Hasse⁴², M. Hatch⁴², J. He^{6,m}, K. Heijhoff³², K. Heinicke¹⁵, R. D. L. Henderson^{63,50}, A. M. Hennequin⁵⁸, K. Hennessy⁵⁴, L. Henry⁴², J. Heuel¹⁴, A. Hicheur², D. Hill⁴³, M. Hilton⁵⁶, S. E. Hollitt¹⁵, R. Hou⁷, Y. Hou⁸, J. Hu¹⁷, J. Hu⁶⁶, W. Hu⁷, X. Hu³, W. Huang⁶, X. Huang⁶⁷, W. Hulsbergen³², R. J. Hunter⁵⁰, M. Hushchyn³⁸, D. Hutchcroft⁵⁴, P. Ibis¹⁵, M. Idzik³⁴, D. Ilin³⁸, P. Ilten⁵⁹, A. Inglessi³⁸, A. Iniukhin³⁸, A. Ishteev³⁸, K. Ivshin³⁸, R. Jacobsson⁴², H. Jage¹⁴, S. Jakobsen⁴², E. Jans³², B. K. Jashal⁴¹, A. Jawahery⁶⁰, V. Jevtic¹⁵, X. Jiang^{4,6}, M. John⁵⁷, D. Johnson⁵⁸, C. R. Jones⁴⁹, T. P. Jones⁵⁰, B. Jost⁴², N. Jurik⁴², S. Kandybei⁴⁵, Y. Kang³, M. Karacson⁴², D. Karpenkov³⁸, M. Karpov³⁸, J. W. Kautz⁵⁹, F. Keizer⁴², D. M. Keller⁶², M. Kenzie⁵⁰, T. Ketel³³, B. Khanji¹⁵, A. Kharisova³⁸, S. Kholodenko³⁸, T. Kirn¹⁴, V. S. Kirsebom⁴³, O. Kitouni⁵⁸, S. Klaver³³, N. Kleijne^{29,c}, K. Klimaszewski³⁶, M. R. Kmiec³⁶, S. Koliiev⁴⁶, A. Kondybayeva³⁸, A. Konoplyannikov³⁸, P. Kopciwicz³⁴, R. Kopecna¹⁷, P. Koppenburg³², M. Korolev³⁸, I. Kostiuk^{32,46}, O. Kot⁴⁶, S. Kotriakhova³⁸, A. Kozachuk³⁸, P. Kravchenko³⁸, L. Kravchuk³⁸, R. D. Krawczyk⁴², M. Kreps⁵⁰, S. Kretzschmar¹⁴, P. Krokovny³⁸, W. Krupa³⁴, W. Krzemien³⁶, J. Kubat¹⁷, W. Kucewicz^{35,34}, M. Kucharczyk³⁵, V. Kudryavtsev³⁸, H. S. Kuindersma³², G. J. Kunde⁶¹, D. Lacarrere⁴², G. Lafferty⁵⁶, A. Lai²⁷, A. Lampis^{27,j}, D. Lancierini⁴⁴, J. J. Lane⁵⁶, R. Lane⁴⁸, G. Lanfranchi²³, C. Langenbruch¹⁴, J. Langer¹⁵, O. Lantwin³⁸, T. Latham⁵⁰, F. Lazzari^{29,n}, M. Lazzaroni^{25,o}, R. Le Gac¹⁰, S. H. Lee⁷⁶, R. Lefèvre⁹, A. Leflat³⁸, S. Legotin³⁸, P. Lenisa^{21,d}, O. Leroy¹⁰, T. Lesiak³⁵, B. Leverington¹⁷, H. Li⁶⁶, K. Li⁷, P. Li¹⁷, S. Li⁷, Y. Li⁴, Z. Li⁶², X. Liang⁶², C. Lin⁶, T. Lin⁵⁵, R. Lindner⁴², V. Lisovskyi¹⁵, R. Litvinov^{27,j}, G. Liu⁶⁶, H. Liu⁶, Q. Liu⁶, S. Liu^{4,6}, A. Lobo Salvia³⁹, A. Loi²⁷, R. Lollini⁷¹, J. Lomba Castro⁴⁰, I. Longstaff⁵³, J. H. Lopes², S. López Soliño⁴⁰, G. H. Lovell⁴⁹, Y. Lu^{4,p}, C. Lucarelli^{22,b}, D. Lucchesi^{28,q}, S. Luchuk³⁸, M. Lucio Martinez³², V. Lukashenko^{32,46}, Y. Luo³, A. Lupato⁵⁶, E. Luppi^{21,d}, A. Lusiani^{29,c}, K. Lynch¹⁸, X.-R. Lyu⁶, L. Ma⁴, R. Ma⁶, S. Maccolini²⁰, F. Machefert¹¹, F. Maciuc³⁷, V. Macko⁴³, P. Mackowiak¹⁵, S. Maddrell-Mander⁴⁸, L. R. Madhan Mohan⁴⁸, A. Maevskiy³⁸, D. Maisuzenko³⁸, M. W. Majewski³⁴, J. J. Malczewski³⁵, S. Malde⁵⁷, B. Malecki³⁵, A. Malinin³⁸, T. Maltsev³⁸, H. Malygina¹⁷, G. Manca^{27,j}, G. Mancinelli¹⁰, D. Manuzzi²⁰, C. A. Manzari⁴⁴, D. Marangotto^{25,o}, J. F. Marchand⁸, U. Marconi²⁰, S. Mariani^{22,b}, C. Marin Benito⁴², M. Marinangeli⁴³, J. Marks¹⁷, A. M. Marshall⁴⁸, P. J. Marshall⁵⁴, G. Martelli^{71,r}, G. Martellotti³⁰, L. Martinazzoli^{42,e}, M. Martinelli^{26,e}, D. Martinez Santos⁴⁰, F. Martinez Vidal⁴¹, A. Massafferri¹, M. Materok¹⁴, R. Matev⁴², A. Mathad⁴⁴, V. Matiunin³⁸, C. Matteuzzi²⁶, K. R. Mattioli⁷⁶, A. Mauri³², E. Maurice¹², J. Mauricio³⁹, M. Mazurek⁴², M. McCann⁵⁵, L. McConnell¹⁸, T. H. McGrath⁵⁶, N. T. McHugh⁵³, A. McNab⁵⁶, R. McNulty¹⁸, J. V. Mead⁵⁴, B. Meadows⁵⁹, G. Meier¹⁵, D. Melnychuk³⁶, S. Meloni^{26,e}, M. Merk^{32,73}, A. Merli^{25,o}, L. Meyer Garcia², M. Mikhasenko^{69,s}, D. A. Milanes⁶⁸, E. Millard⁵⁰, M. Milovanovic⁴², M.-N. Minard^{8,8,a}, A. Minotti^{26,e}, S. E. Mitchell⁵², B. Mitreska⁵⁶, D. S. Mittel¹⁵, A. Mödden¹⁵, R. A. Mohammed⁵⁷, R. D. Moise⁵⁵, S. Mokhnenko³⁸, T. Mombächer⁴⁰, I. A. Monroy⁶⁸, S. Monteil⁹, M. Morandin²⁸, G. Morello²³, M. J. Morello^{29,c}, J. Moron³⁴, A. B. Morris⁶⁹, A. G. Morris⁵⁰, R. Mountain⁶², H. Mu³, F. Muheim⁵², M. Mulder⁷², K. Müller⁴⁴, C. H. Murphy⁵⁷, D. Murray⁵⁶, R. Murta⁵⁵, P. Muzzetto^{27,j}, P. Naik⁴⁸, T. Nakada⁴³, R. Nandakumar⁵¹, T. Nanut⁴², I. Nasteva², M. Needham⁵², N. Neri^{25,o}, S. Neubert⁶⁹, N. Neufeld⁴², P. Neustroev³⁸, R. Newcombe⁵⁵, E. M. Niel⁴³, S. Nieswand¹⁴, N. Nikitin³⁸, N. S. Nolte⁵⁸, C. Normand^{8,27,j}, C. Nunez⁷⁶, A. Oblakowska-Mucha³⁴, V. Obraztsov³⁸, T. Oeser¹⁴, D. P. O'Hanlon⁴⁸, S. Okamura^{21,d}, R. Oldeman^{27,j}, F. Oliva⁵², M. E. Olivares⁶², C. J. G. Onderwater⁷², R. H. O'Neil⁵², J. M. Otalora Goicochea², T. Ovsianikova³⁸, P. Owen⁴⁴, A. Oyanguren⁴¹, O. Ozcelik⁵², K. O. Padenken⁶⁹, B. Pagare⁵⁰, P. R. Pais⁴², T. Pajero⁵⁷, A. Palano¹⁹, M. Palutan²³, Y. Pan⁵⁶, G. Panshin³⁸, A. Papanestis⁵¹, M. Pappagallo^{19,h}, L. L. Pappalardo^{21,d}, C. Pappenheimer⁵⁹, W. Parker⁶⁰, C. Parkes⁵⁶, B. Passalacqua^{21,d}, G. Passaleva²², A. Pastore¹⁹, M. Patel⁵⁵, C. Patrignani^{20,f}, C. J. Pawley⁷³, A. Pearce⁴², A. Pellegrino³², M. Pepe Altarelli⁴², S. Perazzini²⁰, D. Pereima³⁸, A. Pereiro Castro⁴⁰, P. Perret⁹, M. Petric⁵³, K. Petridis⁴⁸, A. Petrolini^{24,g}, A. Petrov³⁸, S. Petrucci⁵², M. Petruzzio²⁵, H. Pham⁶², A. Philippov³⁸, R. Piandani⁶, L. Pica^{29,c}, M. Piccini⁷¹, B. Pietrzyk⁸, G. Pietrzyk¹¹, M. Pili⁵⁷, D. Pinci³⁰, F. Pisani⁴², M. Pizzichemi^{26,42,e}, V. Placinta³⁷, J. Plews⁴⁷, M. Plo Casasus⁴⁰, F. Polci^{13,42}, M. Poli Lener²³, M. Poliakov⁶², A. Poluektov¹⁰, N. Polukhina³⁸, I. Polyakov⁶², E. Polycarpo², S. Ponce⁴², D. Popov^{6,42}, S. Popov³⁸, S. Poslavskii³⁸, K. Prasanth³⁵, L. Promberger⁴², C. Prouve⁴⁰, V. Pugatch⁴⁶, V. Puill¹¹, G. Punzi^{29,t}, H. R. Qi³, W. Qian⁶, N. Qin³, S. Qu³

R. Quagliani⁴³, N. V. Raab¹⁸, R. I. Rabadan Trejo⁶, B. Rachwal³⁴, J. H. Rademacker⁴⁸, R. Rajagopalan,⁶²
M. Rama²⁹, M. Ramos Pernas⁵⁰, M. S. Rangel², F. Ratnikov³⁸, G. Raven^{33,42}, M. Rebollo De Miguel⁴¹,
M. Reboud⁸, F. Redi⁴², F. Reiss⁵⁶, C. Remon Alepuz⁴¹, Z. Ren³, V. Renaudin⁵⁷, P. K. Resmi¹⁰, R. Ribatti^{29,c},
A. M. Ricci²⁷, S. Ricciardi⁵¹, K. Rinnert⁵⁴, P. Robbe¹¹, G. Robertson⁵², A. B. Rodrigues⁴³, E. Rodrigues⁵⁴,
J. A. Rodriguez Lopez⁶⁸, E. Rodriguez Rodriguez⁴⁰, A. Rollings⁵⁷, P. Roloff⁴², V. Romanovskiy³⁸,
M. Romero Lamas⁴⁰, A. Romero Vidal⁴⁰, J. D. Roth,^{76,a} M. Rotondo²³, M. S. Rudolph⁶², T. Ruf⁴²,
R. A. Ruiz Fernandez⁴⁰, J. Ruiz Vidal⁴¹, A. Ryzhikov³⁸, J. Ryzka³⁴, J. J. Saborido Silva⁴⁰, N. Sagidova³⁸,
N. Sahoo⁴⁷, B. Saitta^{27,j}, M. Salomoni⁴², C. Sanchez Gras³², I. Sanderswood⁴¹, R. Santacesaria³⁰,
C. Santamarina Rios⁴⁰, M. Santimaria²³, E. Santovetti^{31,k}, D. Saranin³⁸, G. Sarpis¹⁴, M. Sarpis⁶⁹, A. Sarti³⁰,
C. Satriano^{30,u}, A. Satta³¹, M. Saur¹⁵, D. Savrina³⁸, H. Sazak⁹, L. G. Scantlebury Smead⁵⁷, A. Scarabotto¹³,
S. Schael¹⁴, S. Scherl⁵⁴, M. Schiller⁵³, H. Schindler⁴², M. Schmelling¹⁶, B. Schmidt⁴², S. Schmitt¹⁴,
O. Schneider⁴³, A. Schopper⁴², M. Schubiger³², S. Schulte⁴³, M. H. Schune¹¹, R. Schwemmer⁴²,
B. Sciascia^{23,42}, A. Sciuccati⁴², S. Sellam⁴⁰, A. Semennikov³⁸, M. Senghi Soares³³, A. Sergi^{24,g}, N. Serra⁴⁴,
L. Sestini²⁸, A. Seuthe¹⁵, Y. Shang⁵, D. M. Shangase⁷⁶, M. Shapkin³⁸, I. Shchemerov³⁸, L. Shchutka⁴³,
T. Shears⁵⁴, L. Shekhtman³⁸, Z. Shen⁵, S. Sheng^{4,6}, V. Shevchenko³⁸, E. B. Shields^{26,e}, Y. Shimizu¹¹,
E. Shmanin³⁸, J. D. Shupperd⁶², B. G. Siddi^{21,d}, R. Silva Coutinho⁴⁴, G. Simi²⁸, S. Simone^{19,h}, M. Singla⁶³,
N. Skidmore⁵⁶, R. Skuzia¹⁷, T. Skwarnicki⁶², M. W. Slater⁴⁷, I. Slazyk^{21,d}, J. C. Smallwood⁵⁷, J. G. Smeaton⁴⁹,
E. Smith⁴⁴, M. Smith⁵⁵, A. Snoch³², L. Soares Lavra⁹, M. D. Sokoloff⁵⁹, F. J. P. Soler⁵³, A. Solomin^{38,48},
A. Solovev³⁸, I. Solovyev³⁸, F. L. Souza De Almeida², B. Souza De Paula², B. Spaan^{15,a}, E. Spadaro Norella^{25,o},
E. Spiridenkov³⁸, P. Spradlin⁵³, V. Sriskaran⁴², F. Stagni⁴², M. Stahl⁵⁹, S. Stahl⁴², S. Stanislaus⁵⁷,
O. Steinkamp⁴⁴, O. Stenyakin³⁸, H. Stevens¹⁵, S. Stone^{62,a}, D. Strelkina³⁸, F. Suljik⁵⁷, J. Sun²⁷, L. Sun⁶⁷,
Y. Sun⁶⁰, P. Svihra⁵⁶, P. N. Swallow⁴⁷, K. Swientek³⁴, A. Szabelski³⁶, T. Szumlak³⁴, M. Szymanski⁴²,
S. Taneja⁵⁶, A. R. Tanner⁴⁸, M. D. Tat⁵⁷, A. Terentev³⁸, F. Teubert⁴², E. Thomas⁴², D. J. D. Thompson⁴⁷,
K. A. Thomson⁵⁴, H. Tilquin⁵⁵, V. Tisserand⁹, S. T'Jampens⁸, M. Tobin⁴, L. Tomassetti^{21,d}, X. Tong⁵,
D. Torres Machado¹, D. Y. Tou³, E. Trifonova³⁸, S. M. Trilov⁴⁸, C. Trippel⁴³, G. Tuci⁶, A. Tully⁴³, N. Tuning^{32,42},
A. Ukleja³⁶, D. J. Unverzagt¹⁷, E. Ursov³⁸, A. Usachov³², A. Ustyuzhanin³⁸, U. Uwer¹⁷, A. Vagner³⁸,
V. Vagnoni²⁰, A. Valassi⁴², G. Valenti²⁰, N. Valls Canudas⁷⁴, M. van Beuzekom³², M. Van Dijk⁴³,
H. Van Hecke⁶¹, E. van Herwijnen³⁸, M. van Veghel⁷², R. Vazquez Gomez³⁹, P. Vazquez Regueiro⁴⁰,
C. Vázquez Sierra⁴², S. Vecchi²¹, J. J. Velthuis⁴⁸, M. Veltri^{22,v}, A. Venkateswaran⁶², M. Veronesi³²,
M. Vesterinen⁵⁰, D. Vieira⁵⁹, M. Vieites Diaz⁴³, X. Vilasis-Cardona⁷⁴, E. Vilella Figueras⁵⁴, A. Villa²⁰,
P. Vincent¹³, F. C. Volle¹¹, D. vom Bruch¹⁰, A. Vorobyev³⁸, V. Vorobyev³⁸, N. Voropaev³⁸, K. Vos⁷³, R. Waldi¹⁷,
J. Walsh²⁹, C. Wang¹⁷, J. Wang⁵, J. Wang⁴, J. Wang³, J. Wang⁶⁷, M. Wang⁵, R. Wang⁴⁸, Y. Wang⁷,
Z. Wang⁴⁴, Z. Wang³, Z. Wang⁶, J. A. Ward^{50,63}, N. K. Watson⁴⁷, D. Websdale⁵⁵, C. Weisser⁵⁸,
B. D. C. Westhenry⁴⁸, D. J. White⁵⁶, M. Whitehead⁵³, A. R. Wiederhold⁵⁰, D. Wiedner¹⁵, G. Wilkinson⁵⁷,
M. K. Wilkinson⁵⁹, I. Williams⁴⁹, M. Williams⁵⁸, M. R. J. Williams⁵², F. F. Wilson⁵¹, W. Wislicki³⁶, M. Witek³⁵,
L. Witola¹⁷, C. P. Wong⁶¹, G. Wormser¹¹, S. A. Wotton⁴⁹, H. Wu⁶², K. Wyllie⁴², Z. Xiang⁶, D. Xiao⁷,
Y. Xie⁷, A. Xu⁵, J. Xu⁶, L. Xu³, M. Xu⁵⁰, Q. Xu⁶, Z. Xu⁹, Z. Xu⁶, D. Yang³, S. Yang⁶, Y. Yang⁶,
Z. Yang⁵, Z. Yang⁶⁰, Y. Yao⁶², L. E. Yeomans⁵⁴, H. Yin⁷, J. Yu⁶⁵, X. Yuan⁶², E. Zaffaroni⁴³, M. Zavertyaev¹⁶,
M. Zdybal³⁵, O. Zenaiev⁴², M. Zeng³, D. Zhang⁷, L. Zhang³, S. Zhang⁶⁵, S. Zhang⁵, Y. Zhang⁵, Y. Zhang⁵⁷,
A. Zharkova³⁸, A. Zhelezov¹⁷, Y. Zheng⁶, T. Zhou⁵, X. Zhou⁶, Y. Zhou⁶, V. Zhovkovska¹¹, X. Zhu³,
X. Zhu⁷, Z. Zhu⁶, V. Zhukov^{14,38}, Q. Zou^{4,6}, S. Zucchelli^{20,f}, D. Zuliani²⁸ and G. Zunica⁵⁶

(LHCb Collaboration)

¹Centro Brasileiro de Pesquisas Físicas (CBPF), Rio de Janeiro, Brazil

²Universidade Federal do Rio de Janeiro (UFRJ), Rio de Janeiro, Brazil

³Center for High Energy Physics, Tsinghua University, Beijing, China

⁴Institute Of High Energy Physics (IHEP), Beijing, China

⁵School of Physics State Key Laboratory of Nuclear Physics and Technology, Peking University, Beijing, China

- ⁶University of Chinese Academy of Sciences, Beijing, China
- ⁷Institute of Particle Physics, Central China Normal University, Wuhan, Hubei, China
- ⁸Université Savoie Mont Blanc, CNRS, IN2P3-LAPP, Annecy, France
- ⁹Université Clermont Auvergne, CNRS/IN2P3, LPC, Clermont-Ferrand, France
- ¹⁰Aix Marseille Univ, CNRS/IN2P3, CPPM, Marseille, France
- ¹¹Université Paris-Saclay, CNRS/IN2P3, IJCLab, Orsay, France
- ¹²Laboratoire Leprince-Ringuet, CNRS/IN2P3, Ecole Polytechnique, Institut Polytechnique de Paris, Palaiseau, France
- ¹³LPNHE, Sorbonne Université, Paris Diderot Sorbonne Paris Cité, CNRS/IN2P3, Paris, France
- ¹⁴I. Physikalisches Institut, RWTH Aachen University, Aachen, Germany
- ¹⁵Fakultät Physik, Technische Universität Dortmund, Dortmund, Germany
- ¹⁶Max-Planck-Institut für Kernphysik (MPIK), Heidelberg, Germany
- ¹⁷Physikalisches Institut, Ruprecht-Karls-Universität Heidelberg, Heidelberg, Germany
- ¹⁸School of Physics, University College Dublin, Dublin, Ireland
- ¹⁹INFN Sezione di Bari, Bari, Italy
- ²⁰INFN Sezione di Bologna, Bologna, Italy
- ²¹INFN Sezione di Ferrara, Ferrara, Italy
- ²²INFN Sezione di Firenze, Firenze, Italy
- ²³INFN Laboratori Nazionali di Frascati, Frascati, Italy
- ²⁴INFN Sezione di Genova, Genova, Italy
- ²⁵INFN Sezione di Milano, Milano, Italy
- ²⁶INFN Sezione di Milano-Bicocca, Milano, Italy
- ²⁷INFN Sezione di Cagliari, Monserrato, Italy
- ²⁸Università degli Studi di Padova, Università e INFN, Padova, Padova, Italy
- ²⁹INFN Sezione di Pisa, Pisa, Italy
- ³⁰INFN Sezione di Roma La Sapienza, Roma, Italy
- ³¹INFN Sezione di Roma Tor Vergata, Roma, Italy
- ³²Nikhef National Institute for Subatomic Physics, Amsterdam, Netherlands
- ³³Nikhef National Institute for Subatomic Physics and VU University Amsterdam, Amsterdam, Netherlands
- ³⁴AGH - University of Science and Technology, Faculty of Physics and Applied Computer Science, Kraków, Poland
- ³⁵Henryk Niewodniczanski Institute of Nuclear Physics Polish Academy of Sciences, Kraków, Poland
- ³⁶National Center for Nuclear Research (NCBJ), Warsaw, Poland
- ³⁷Horia Hulubei National Institute of Physics and Nuclear Engineering, Bucharest-Magurele, Romania
- ³⁸Affiliated with an institute covered by a cooperation agreement with CERN
- ³⁹ICCUB, Universitat de Barcelona, Barcelona, Spain
- ⁴⁰Instituto Galego de Física de Altas Enerxías (IGFAE), Universidade de Santiago de Compostela, Santiago de Compostela, Spain
- ⁴¹Instituto de Física Corpuscular, Centro Mixto Universidad de Valencia - CSIC, Valencia, Spain
- ⁴²European Organization for Nuclear Research (CERN), Geneva, Switzerland
- ⁴³Institute of Physics, Ecole Polytechnique Fédérale de Lausanne (EPFL), Lausanne, Switzerland
- ⁴⁴Physik-Institut, Universität Zürich, Zürich, Switzerland
- ⁴⁵NSC Kharkiv Institute of Physics and Technology (NSC KIPT), Kharkiv, Ukraine
- ⁴⁶Institute for Nuclear Research of the National Academy of Sciences (KINR), Kyiv, Ukraine
- ⁴⁷University of Birmingham, Birmingham, United Kingdom
- ⁴⁸H.H. Wills Physics Laboratory, University of Bristol, Bristol, United Kingdom
- ⁴⁹Cavendish Laboratory, University of Cambridge, Cambridge, United Kingdom
- ⁵⁰Department of Physics, University of Warwick, Coventry, United Kingdom
- ⁵¹STFC Rutherford Appleton Laboratory, Didcot, United Kingdom
- ⁵²School of Physics and Astronomy, University of Edinburgh, Edinburgh, United Kingdom
- ⁵³School of Physics and Astronomy, University of Glasgow, Glasgow, United Kingdom
- ⁵⁴Oliver Lodge Laboratory, University of Liverpool, Liverpool, United Kingdom
- ⁵⁵Imperial College London, London, United Kingdom
- ⁵⁶Department of Physics and Astronomy, University of Manchester, Manchester, United Kingdom
- ⁵⁷Department of Physics, University of Oxford, Oxford, United Kingdom
- ⁵⁸Massachusetts Institute of Technology, Cambridge, MA, United States
- ⁵⁹University of Cincinnati, Cincinnati, OH, United States
- ⁶⁰University of Maryland, College Park, MD, United States
- ⁶¹Los Alamos National Laboratory (LANL), Los Alamos, NM, United States
- ⁶²Syracuse University, Syracuse, NY, United States
- ⁶³School of Physics and Astronomy, Monash University, Melbourne, Australia
(associated with Department of Physics, University of Warwick, Coventry, United Kingdom)

⁶⁴*Pontifícia Universidade Católica do Rio de Janeiro (PUC-Rio), Rio de Janeiro, Brazil
(associated with Universidade Federal do Rio de Janeiro (UFRJ), Rio de Janeiro, Brazil)*

⁶⁵*Physics and Micro Electronic College, Hunan University, Changsha City, China
(associated with Institute of Particle Physics, Central China Normal University, Wuhan, Hubei, China)*

⁶⁶*Guangdong Provincial Key Laboratory of Nuclear Science, Guangdong-Hong Kong Joint Laboratory of Quantum Matter,
Institute of Quantum Matter, South China Normal University, Guangzhou, China*

(associated with Center for High Energy Physics, Tsinghua University, Beijing, China)

⁶⁷*School of Physics and Technology, Wuhan University, Wuhan, China
(associated with Center for High Energy Physics, Tsinghua University, Beijing, China)*

⁶⁸*Departamento de Física, Universidad Nacional de Colombia, Bogota, Colombia
(associated with LPNHE, Sorbonne Université, Paris Diderot Sorbonne Paris Cité, CNRS/IN2P3, Paris, France)*

⁶⁹*Universität Bonn - Helmholtz-Institut für Strahlen und Kernphysik, Bonn, Germany
(associated with Physikalisches Institut, Ruprecht-Karls-Universität Heidelberg, Heidelberg, Germany)*

⁷⁰*Eotvos Lorand University, Budapest, Hungary
(associated with European Organization for Nuclear Research (CERN), Geneva, Switzerland)*

⁷¹*INFN Sezione di Perugia, Perugia, Italy
(associated with INFN Sezione di Ferrara, Ferrara, Italy)*

⁷²*Van Swinderen Institute, University of Groningen, Groningen, Netherlands
(associated with Nikhef National Institute for Subatomic Physics, Amsterdam, Netherlands)*

⁷³*Universiteit Maastricht, Maastricht, Netherlands
(associated with Nikhef National Institute for Subatomic Physics, Amsterdam, Netherlands)*

⁷⁴*DS4DS, La Salle, Universitat Ramon Llull, Barcelona, Spain
(associated with ICCUB, Universitat de Barcelona, Barcelona, Spain)*

⁷⁵*Department of Physics and Astronomy, Uppsala University, Uppsala, Sweden
(associated with School of Physics and Astronomy, University of Glasgow, Glasgow, United Kingdom)*

⁷⁶*University of Michigan, Ann Arbor, MI, United States
(associated with Syracuse University, Syracuse, NY, United States)*

^aDeceased.

^bAlso at Università di Firenze, Firenze, Italy.

^cAlso at Scuola Normale Superiore, Pisa, Italy.

^dAlso at Università di Ferrara, Ferrara, Italy.

^eAlso at Università di Milano Bicocca, Milano, Italy.

^fAlso at Università di Bologna, Bologna, Italy.

^gAlso at Università di Genova, Genova, Italy.

^hAlso at Università di Bari, Bari, Italy.

ⁱAlso at Universidad Nacional Autónoma de Honduras, Tegucigalpa, Honduras.

^jAlso at Università di Cagliari, Cagliari, Italy.

^kAlso at Università di Roma Tor Vergata, Roma, Italy.

^lAlso at Universidade Federal do Triângulo Mineiro (UFTM), Uberaba-MG, Brazil.

^mAlso at Hangzhou Institute for Advanced Study, UCAS, Hangzhou, China.

ⁿAlso at Università di Siena, Siena, Italy.

^oAlso at Università degli Studi di Milano, Milano, Italy.

^pAlso at Central South U., Changsha, China.

^qAlso at Università di Padova, Padova, Italy.

^rAlso at Università di Perugia, Perugia, Italy.

^sAlso at Excellence Cluster ORIGINS, Munich, Germany.

^tAlso at Università di Pisa, Pisa, Italy.

^uAlso at Università della Basilicata, Potenza, Italy.

^vAlso at Università di Urbino, Urbino, Italy.